PSFC/JA-08-29

Oblique Ion Collection in the Drift-Approximation: How Magnetized Mach-Probes Really Work

I.H. Hutchinson

September 2008

Plasma Science and Fusion Center
Massachusetts Institute of Technology
Cambridge MA 02139 USA

Submitted for publication to Physics of Plasmas.

Oblique ion collection in the drift-approximation: how magnetized Mach-probes really work.

I H Hutchinson

Plasma Science and Fusion Center and
Department of Nuclear Science and Engineering,
Massachusetts Institute of Technology,
Cambridge, MA 02139, USA

September 17, 2008

Abstract

The anisotropic fluid equations governing a frictionless obliquely-flowing plasma around an essentially arbitrarily shaped three-dimensional ion-absorbing object in a strong magnetic field are solved analytically in the quasi-neutral drift-approximation, neglecting parallel temperature gradients. The effects of transverse displacements traversing the magnetic presheath are also quantified. It is shown that the parallel collection flux density dependence upon external Mach-number is $n_\infty c_s \exp[-1 - (M_{\|\infty} - M_\perp \cot\theta)]$ where θ is the angle (in the plane of field and drift velocity) of the object-surface to the magnetic-field and $M_{\|\infty}$ is the external parallel flow. The perpendicular drift, $\mathbf{M}_\perp$, appearing here consists of the external $\mathbf{E} \wedge \mathbf{B}$ drift plus a weighted sum of the ion and electron diamagnetic drifts that depends upon the total angle of the surface to the magnetic field. It is that somewhat counter-intuitive combination that an oblique (transverse) Mach probe experiment measures.

Ion collection by solid objects immersed in a plasma is a problem of perennial interest in plasma physics. It provides the basis for the measurement of plasma parameters by electric (Langmuir) probes[1] as well as the charging of dust[2] and spacecraft[3]. The present work addresses the situation where the ion Larmor radius (in the background magnetic field $\mathbf{B}$) is much smaller than the object, so that perpendicular plasma flow is strongly constrained.

This problem has important similarities to the solution of the flow of plasma to a plane aligned obliquely to the field, the most obvious example being a tokamak divertor plate. That problem can be formulated[4] as one-dimensional, taking the coordinates in the plane as being ignorable. However, it is well established that no spatially-varying solution of the quasi-neutral plasma equations in one dimension is possible without additional sources of particles (e.g. through ionization) or momentum (e.g. from collisions). Recent studies of this problem of the one-dimensional magnetized plasma and oblique presheath (e.g. [5, 6]) have

1

mostly focussed on collisions as the mechanism allowing the acceleration of the plasma into the magnetic presheath. For localized probes, however, if one conceptualizes the problem as being dominated by the one-dimensional dynamics along the field, the *cross-field flux divergence* is the most natural effective source to permit parallel gradients.

Prior theoretical probe studies have focussed on situations where the cross-field magnetized-ion flux can be described (somewhat phenomenologically) as *diffusive*. The full numerical solutions for this formulation [7, 8] yield the dependence of the collected ion flux density on the plasma density and temperature, and the parallel (to $\mathbf{B}$) Mach-number. That provides the theoretical calibration factor for a (parallel) Mach-probe (a probe with electrodes facing parallel and anti-parallel to the field), when the perpendicular drift velocity is ignorable. This "calibration" proves to be in good agreement with independent measurements and calculations [9] and has been widely adopted for experimental interpretation.

The approximate one-dimensional diffusive treatment has been generalized[10] to include an additional perpendicular plasma drift velocity, accounting for the boundary-condition modification[11] that the transverse drift causes. Measuring the dependence of the ion collection current-density on orientation of oblique probe faces then allows one to deduce the perpendicular as well as the parallel external drift velocity. The generalized solution can be shown[1] to be a simple Galilean transformation of the solution for zero transverse drift, which incidentally reminds us of the elementary physical equivalence of $\mathbf{E} \wedge \mathbf{B}$ drift past a fixed object and motion of the object through a stationary plasma. The equivalence also indicates, though, that the generalized diffusion solution is rigorously valid only for an oblique surface of effectively infinite dimension in the transverse drift direction (so that the Galilean equivalence in this direction is valid), but finite in the direction perpendicular to both flow and magnetic field (so that diffusion in this perpendicular direction dominates the cross-field divergence). Practical Mach-probes generally do not have this configuration. They are more often multi-faceted 'Gundestrup' types[12, 13, 14], where many short adjacent collectors are used with different orientations. So it is not obvious that the generalized diffusive solution applies.

In fact, when there is substantial pre-existing cross-field drift of the ions, it is perhaps physically more reasonable to regard that drift as the dominant cross-field transport mechanism, and to *ignore diffusion*. Gunn [15, 9] has explored this problem, with a uniform impressed cross-field drift, in two dimensions with his particle-in-cell code. This drift physics is appropriate to many space and astrophysical problems too; for example to the interaction of Jupiter's satellites with its magnetosphere. It is the purpose of the present work to derive a general analytic (3-dimensional) solution to this purely advective problem, with fully self-consistent drift velocity.

First, to introduce the solution by characteristics, we recall a recent complete exact solution to this problem[16] for an arbitrary shaped probe under the model ansatz that the perpendicular drift velocity is uniform. This is a generalization of an earlier self-similar solution[17] mathematically equivalent to a one-dimensional free expansion into a vacuum. The very simple general analytic result obtained for the ion flux is gratifyingly close to the diffusive-plasma result, and hence to the PIC calculations of Gunn (which include full ion

distribution-function parallel gradients). The solution demonstrates that provided the probe is convex, the flux is not affected (for negligible Larmor radius) by spatial derivatives of the surface angle in the drift-direction. The uniform drift ansatz is justified by inspection only when the probe is two-dimensional; so that the coordinate perpendicular to the field and drift is ignorable and the probe-perturbation of the plasma does not introduce additional drifts except along the ignorable coordinate. Again, practical probes are generally not well-approximated as two-dimensional, so the question remains as to whether that uniform-drift-velocity solution applies in practice.

The following remarkable result is rigorously demonstrated in section 3. The ion flux to the probe surfaces derived for uniform-drift-velocity *does* apply even when the full spatially-varying self-consistent drift velocity, including the perturbation from an arbitrarily-shaped three-dimensional probe, is accounted for. When the external drift arises purely from electric field, one can obtain the full self-consistent spatial dependence of the density and velocity throughout the perturbed plasma region, using an elementary geometric algorithm. Some examples are given.

Furthermore, external *diamagnetic drifts* can also be included, again for arbitrary-shaped three-dimensional probes. They make important but counterintuitive contributions to the observed ion current density. In addition to the effects that arise in the plasma, it is essential to account for transverse displacements that arise in the magnetic presheath; they are calculated in section 4. Such local drifts in the magnetic presheath have previously been identified[18, 19] as important contributors to oblique boundary conditions. The present work provides a more general solution of the magnetic presheath displacement effects, dispensing with small-angle approximations.

The final result is that a transverse Mach-probe measures effectively the sum of the external $\mathbf{E} \wedge \mathbf{B}$ drift and a combination of the ion and electron diamagnetic drifts. At small angles between the field and the collector, the dominant diamagnetic term is the *electron* diamagnetic drift, which of course is generally in the opposite direction to the ion diamagnetic drift.

The presheath displacements can give rise to bias in Mach probe measurements. Its relative magnitude is of order the ratio of Larmor radius to electrode size. The effects of orthogonal displacements in the plasma region are also calculated rigorously. They modify the expression for the flux in ways that are usually of little importance for practical measurements.

1 Formulation

We analyse the dynamics of the ion-fluid through the steady-state continuity and momentum equations

$$\nabla.(n\mathbf{v}) = 0 \tag{1}$$

$$mn(\mathbf{v}.\nabla)\mathbf{v} = -nZe\nabla\phi - \nabla p + nZe(\mathbf{v} \wedge \mathbf{B}) , \tag{2}$$

where m, Z, n, p, T_i, $\mathbf{v}$ are the ion mass, charge-number, density, pressure, temperature, and velocity, and ϕ is the potential. We split the momentum equation into the components parallel ($\parallel$) and perpendicular ($\perp$) to the (assumed uniform) magnetic field, and take the cross-product with $\mathbf{B}$ of the perpendicular part to obtain the form

$$\mathbf{v}_\perp = -\left[\left(\nabla_\perp \phi + \frac{1}{nZe}\nabla_\perp p\right) + \frac{m}{Ze}(\mathbf{v}.\nabla)\mathbf{v}_\perp\right] \wedge \frac{\mathbf{B}}{B^2} \;. \tag{3}$$

We can immediately identify the first two terms in this expression as the $\mathbf{E} \wedge \mathbf{B}$ and diamagnetic drifts. The last term can be considered to be the polarization drift, which we will regard as ignorable. The approximation of omitting the polarization drift requires the Larmor radius to be small c.f. the perpendicular scale-length, generally the probe dimensions. It can be shown by *a posteriori* calculation that the polarization drift is smaller than the imposed perpendicular drift by a factor that is second-order in the Larmor radius. Ignoring the polarization drift term is the meaning here of the expression "drift-approximation". By taking $\mathbf{B}$ to be uniform we have of course eliminated the grad-B and curvature drifts. We adopt the simplest possible fluid closure scheme, that the ion temperature, T_i, is invariant, so that the pressure is simply proportional to density. Together with dropping the the polarization drift, this makes $\mathbf{v}_\perp$ divergenceless:

$$\mathbf{v}_\perp = -\left(\nabla_\perp \phi + \frac{1}{nZe}\nabla_\perp p\right) \wedge \frac{\mathbf{B}}{B^2} = -\nabla_\perp\left(\phi + \frac{T_i}{Ze}\ln n\right) \wedge \frac{\mathbf{B}}{B^2} \;. \tag{4}$$

Under these approximations the continuity and parallel-momentum equations become

$$(\mathbf{v}.\nabla)\ln n + \nabla_\parallel v_\parallel = 0 \tag{5}$$

$$(\mathbf{v}.\nabla)v_\parallel + \frac{Ze}{m}\nabla_\parallel\left(\phi + \frac{T_i}{Ze}\ln n\right) = 0 \;, \tag{6}$$

while the perpendicular-momentum conservation is expressed by the drift $\mathbf{v}_\perp$ expression.

The potential is eliminated from these equations by accounting for the self-consistent solution of the electric field arising from the ion and electron densities. The electron density response along the magnetic field is, as usual, taken to involve rapid equilibration; so that the electron pressure gradient is balanced by electric field:

$$\nabla_\parallel \phi = (T_e/e)\nabla_\parallel \ln n_e \;, \tag{7}$$

where the parallel gradient of the electron temperature, $\nabla_\parallel T_e$, is taken to be zero and the electron density is n_e. Assuming that the Debye length is much smaller than the probe, we will treat the plasma as quasi-neutral, so that $n_e = Zn$.

Using the notation $c_s^2 \equiv (ZT_e + T_i)/m$ and $\mathbf{M} \equiv \mathbf{v}/c_s$, the ion equations then take the normalized form:

$$\mathbf{M}.\nabla \ln n + \nabla_\parallel M_\parallel = 0 \tag{8}$$

$$\mathbf{M}.\nabla M_\parallel + \nabla_\parallel \ln n = 0 \;, \tag{9}$$

4

which can be rearranged by adding and subtracting to show explicitly the "characteristics" [20]

$$(\mathbf{M}.\nabla + \nabla_{\|})(\ln n + M_{\|}) = 0 \tag{10}$$
$$(\mathbf{M}.\nabla - \nabla_{\|})(\ln n - M_{\|}) = 0 . \tag{11}$$

Thus the quantities $(\ln n \pm M_{\|})$ are constant along their corresponding characteristics $d\mathbf{x} = (\mathbf{M} \pm \mathbf{B}/B)ds$. And we can fully solve the problem by analysis of the characteristics.

2   Uniform perpendicular-velocity ansatz

First we review the solution under the condition that the perpendicular velocity is simply a constant, $\mathbf{M}_{\perp}$, independent of space. This ansatz is clearly justified if the coordinate perpendicular to $\mathbf{B}$ and $\mathbf{M}_{\perp}$ is ignorable. See ref [16] for additional details and explanation of the following derivation. We choose axes such that $\mathbf{B}$ is aligned along x and $\mathbf{M}_{\perp} = M_h\hat{\mathbf{y}}$ along y. The requirements expressed by the characteristics (10, 11) are that both

$$(\ln n + M_{\|}) = const \quad \text{along } dx = dy(M_{\|} + 1)/M_h, \tag{12}$$

and

$$(\ln n - M_{\|}) = const \quad \text{along } dx = dy(M_{\|} - 1)/M_h. \tag{13}$$

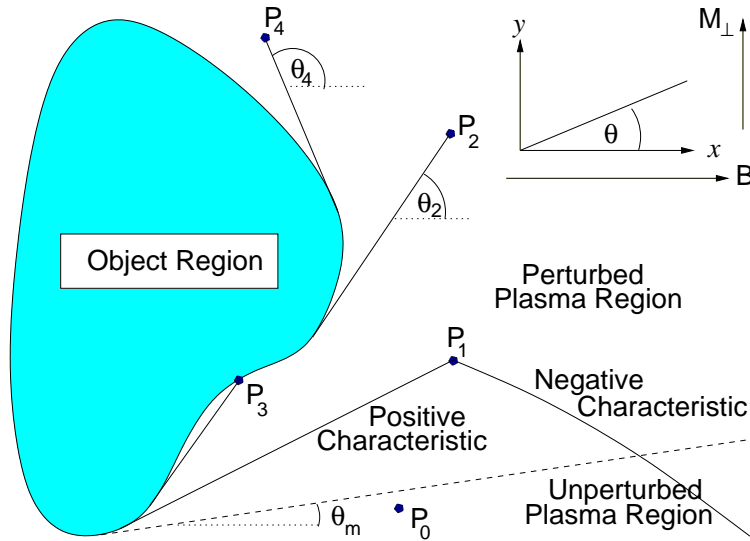These will be referred to respectively as the positive and negative characteristics.

Figure 1: Construction of the solutions at different points. P_0 is in the unperturbed region. For P_1 the characteristics are shown. P_3 is in a concave region and so its positive characteristic is not tangent at P_3. A value $\theta > \pi/2$ such as for P_4 is not problematic.

For definiteness, we now consider plasma that is on the higher-x side (to the right) of the object. Figure 1 will be used for illustration. For any point in the plasma, a positive and a

negative characteristic pass through it. If both characteristics originate in the unperturbed plasma at $y \to -\infty$, and do not enclose the object, then values at the point satisfy both $\ln n + M_\parallel = \ln n_\infty + M_\infty$ and $\ln n - M_\parallel = \ln n_\infty - M_{\parallel\infty}$ (where $_\infty$ indicates values in the unperturbed region). These simultaneous equations have only one solution: $n = n_\infty$, $M_\parallel = M_{\parallel\infty}$, showing that the point is in the unperturbed region, for example: P_0. The characteristics for such points are straight lines with slopes $M_h/(M_{\parallel\infty} \pm 1)$.

The most important case is when just one of the characteristics originates not at $y = -\infty$, but on the surface of the object (e.g. P_1). The positive characteristic is always to the left of the negative characteristic, when tracing backward from a common point. So the characteristic that originates on the object is the positive one. On that characteristic, $(\ln n + M_\parallel)$ is constant, but not equal to the unperturbed value. Each point along the positive characteristic satisfies also $\ln n - M_\parallel = \ln n_\infty - M_{\parallel\infty}$ because there are negative characteristics from infinity to each point. The only way to satisfy these two requirements is that, along the positive characteristic, $M_\parallel = const$ and $n = const$. If $M_\parallel = const$, then the slope of the characteristic, $M_h/(M_\parallel + 1)$ is constant. It is a straight line.

The line's slope is determined by the absorbing boundary condition at the plasma edge. That condition requires[16] $M_\parallel$ to be as negative as possible consistent with the overall solution, which requires the greatest possible slope-angle $\theta \equiv \arctan[M_h/(M_\parallel + 1)]$ (even perhaps such that $\theta > \pi/2$). The characteristic must therefore always be *tangential* to the object boundary where it intersects it. Thus, all positive characteristics that originate on the boundary do so as tangents, and for any point in the perturbed plasma region *the positive characteristic is that straight line passing through the point which has greatest θ and originates as a tangent on the object*. Once that line is determined geometrically, its slope determines $M_\parallel$ and hence n at all points along it. If the steepest tangent angle is less than $\theta_m = \arctan[M_h/(M_{\parallel\infty} + 1)]$, then the positive characteristic does not intersect the object, but has slope $\theta = \theta_m$; and the point is in unperturbed plasma. The entire solution for the plasma in the perturbed neighborhood of an arbitrary-shaped object is thus

$$n = n_\infty \exp(M_\parallel - M_{\parallel\infty}), \quad M_\parallel = M_h \cot\theta - 1. \tag{14}$$

The solution (14) provides an extremely simple formula for the ion flux to a surface not affected by concavity. Adding the perpendicular and parallel components, the total flux density along the outward normal within the (x, y)-plane, i.e. in the direction $(-\sin\theta, \cos\theta)$, is $nc_s(M_h\cos\theta - M_\parallel\sin\theta) = nc_s\sin\theta$. Written as flux per unit area perpendicular to the magnetic field, this is

$$\Gamma_\parallel = n_\infty c_s \exp[-1 - (M_{\parallel\infty} - M_h\cot\theta)]. \tag{15}$$

First, this form indicates, importantly, that for points not in a concave region of the object, the collected flux depends only on the angle of the surface there, and not on the shape of the object at smaller y. Second, the exponential dependence upon $M_{\parallel\infty}$ is within 10% of the dependence, $\exp[-1 - 1.1(M_{\parallel\infty} - M_h\cot\theta)]$, that fits the diffusive solution[10, 1]. Third, consideration of the characteristics shows unambiguously that leading faces, for which $\theta < \theta_m$ receive simply the unperturbed flux $[\Gamma_\parallel = n_\infty c_s(M_h\cot\theta - M_{\parallel\infty})]$, while trailing faces,

6

even those for which $M_{\parallel\infty} - M_h \cot\theta > 1$, are governed by the formula (15). The boundary condition at the magnetic presheath edge is just the same as what is sometimes called the "magnetized Bohm condition" but arises here naturally from the analysis of the quasi-neutral equations.

In a concave region of the object, e.g. at P_3, the surface angle (local tangent) θ_s, is smaller than the characteristic's angle θ, and the distinction must be retained. This leads to an enhanced ion flux, equal to equation (15) times the extra factor $(M_h \cot\theta_s - M_h \cot\theta + 1)$.

3 Accounting for self-consistent drifts

The presence of the probe perturbs the plasma potential and density, for example as calculated in the model case of the previous section. Most probes are of limited extent in the direction (z) perpendicular to the plane containing $\mathbf{B}$ and $\mathbf{M}_{\perp\infty}$, and indeed may have a non-zero z-component of the normal to the collecting surface. The plasma perturbations therefore give rise to spatially-varying ion drifts that frequently break the (z-translational) symmetry assumption used to justify the homogeneous-$\mathbf{M}_\perp$ ansatz. So we must now return to the full equations (10, 11) accounting for the complete, self-consistent, spatially-varying, perpendicular velocity.

The interesting case is of points for which (only) one of the characteristics starts not at infinity but on the probe itself. As before, for definiteness, but without loss of generality, we will take that to be the positive characteristic. At this point then $(\ln n + M_\parallel) \neq (\ln n_\infty + M_{\parallel\infty})$; nevertheless, because of the negative characteristic, it is still true that $(\ln n - M_\parallel) = (\ln n_\infty - M_{\parallel\infty}) = const$. This shows that in a region whose points have any characteristic starting at infinity, the nature of the solution is of the form $M_\parallel = M_\parallel(n)$, and especially $\nabla M_\parallel$ is parallel to ∇n. Consequently if there is a self-consistent combination of density and velocity fields $\{n, M_\parallel, \mathbf{M}_\perp = \mathbf{M}_{\perp 0}\}$ that satisfies the advection equations (10, 11) (and the drift equation, 4), any perpendicular vector field, $\mathbf{M}_{\perp 1}$, that satisfies $\mathbf{M}_{\perp 1}.\nabla n = 0$, also satisfies $\mathbf{M}_{\perp 1}.\nabla M_\parallel = 0$. We can therefore subtract any such $\mathbf{M}_{\perp 1}$ from $\mathbf{M}_\perp$ without affecting the characteristic equations (10, 11). In other words, the combination $\{n, M_\parallel, \mathbf{M}_\perp = (\mathbf{M}_{\perp 0} - \mathbf{M}_{\perp 1})\}$ *also* satisfies the characteristic equations (though not the drift equation, 4). Moreover, the subtraction of $\mathbf{M}_{\perp 1}$ leaves the boundary condition at the plasma edge invariant provided probe curvature is small compared with $1/\rho_s$. The invariance follows from the boundary condition being that the positive characteristic be tangent to the surface. If the surface is expressed by the equation $s(x, y, z) = 0$, then tangency is $d\mathbf{x}.\nabla s = 0$, which along the characteristic is $(M_\parallel + 1)\nabla_\parallel s + \mathbf{M}_\perp.\nabla_\perp s = 0$. In so far as ∇s and ∇n are parallel (i.e. the density is invariant in the tangential directions) subtracting $\mathbf{M}_{\perp 1}$ leaves this condition unchanged. But n is indeed invariant along the surface when given by eq (14) provided that the surface angle (θ_s) gradient (i.e. curvature) can be ignored.

The significance of these observations is profound. It means that although the actual perpendicular velocity $\mathbf{M}_\perp$ may be very complicated, and include drifts arising from the self-consistent potential- and density-gradients caused by the presence of the probe, we do not have to solve the associated complicated characteristics. Instead, we can subtract from

$\mathbf{M}_\perp$ any drift that satisfies $\mathbf{M}_{\perp1}.\nabla n = 0$, and solve the resulting simpler characteristics. The resulting solution for n and $M_\parallel$ is correct then also for the full drift $\mathbf{M}_\perp$ expression.

3.1 Pure $\mathbf{E} \wedge \mathbf{B}$ external drift

Consider first the case when the unperturbed plasma has uniform density ($n_\infty = const$) as well as temperature, but has a uniform impressed perpendicular electric field in the z-direction perpendicular to the field , ($\mathbf{B}/B = \hat{\mathbf{x}}$), giving rise to an $\mathbf{E} \wedge \mathbf{B}$ drift. In other words, we have a non-uniform potential, $\phi_\infty(z)$, such that $\nabla\phi_\infty = -\hat{\mathbf{z}}E$; so that the homogenous drift is $\mathbf{v}_h = \hat{\mathbf{y}}E/B = \mathbf{M}_h c_s$.

In the presence of the probe, the electron parallel momentum (force-balance) equation can be integrated along the field, from infinity to any position to give the perturbed potential

$$\phi - \phi_\infty(z) = (T_e/e)\ln(n/n_\infty) . \tag{16}$$

We substitute this into the drift expression to get

$$\mathbf{v}_\perp = -\nabla\left(\phi_\infty + \frac{T_e}{e}\ln(n/n_\infty) + \frac{T_i}{Ze}\ln n\right) \wedge \frac{\mathbf{B}}{B^2} \tag{17}$$

$$= -\left(\nabla\phi_\infty + \frac{mc_s^2}{Ze}\nabla\ln n\right) \wedge \frac{\mathbf{B}}{B^2} . \tag{18}$$

Or, in normalized form:

$$\mathbf{M}_\perp = \mathbf{M}_h - \rho_s\nabla\ln n \wedge \mathbf{B}/B , \tag{19}$$

where ρ_s is the ion Larmor radius at the sound speed. The perpendicular drift velocity thus consists of a uniform term $\mathbf{M}_h$, equal to the external drift, plus a term $\mathbf{M}_{\perp1}$ ($= -\rho_s\nabla\ln n \wedge \mathbf{B}/B$) arising from local gradients of density (and associated potential), which satisfies $\mathbf{M}_{\perp1}.\nabla n = 0$. Our approach is therefore to solve along characteristics defined not by the complicated full drift velocity $\mathbf{M}_\perp$, but using the uniform external drift velocity $\mathbf{M}_h$ which arises from subtracting off $\mathbf{M}_{\perp1}$, as we have shown we are permitted to do because $\mathbf{M}_{\perp1}.\nabla n = 0$. But such an approach, of using a uniform impressed perpendicular drift, is precisely the ansatz solved in the previous section, albeit without this detailed justification. Therefore, the solution obtained there applies without modification. What *is* modified is that the condition of translational invariance in the orthogonal (z-) direction is removed. In other words, the restriction that the probe be two-dimensional, which was invoked previously to justify the neglect of the density-gradient-induced drifts is proven here to be unnecessary. The results of that section, the dependence of n on $M_\parallel$, the spatial variation of $M_\parallel$ embodied in the equation $\tan\theta = M_h/(M_\parallel + 1)$, and the surface flux expression, apply to any shape of three-dimensional probe, provided only that the condition of convexity (that the surface is not reentrant) is satisfied. This convexity condition must be applied along the original characteristic (before subtracting $\mathbf{M}_{\perp\infty}$) so it depends on the full 3-D shape of the probe (and the z-drifts).

The flux-density of ions from the plasma to the probe surface in this case is given by the vector sum of $\mathbf{M}_h$ and $M_\parallel$ because the additional term $\mathbf{M}_{\perp1}$ is always locally tangential

8

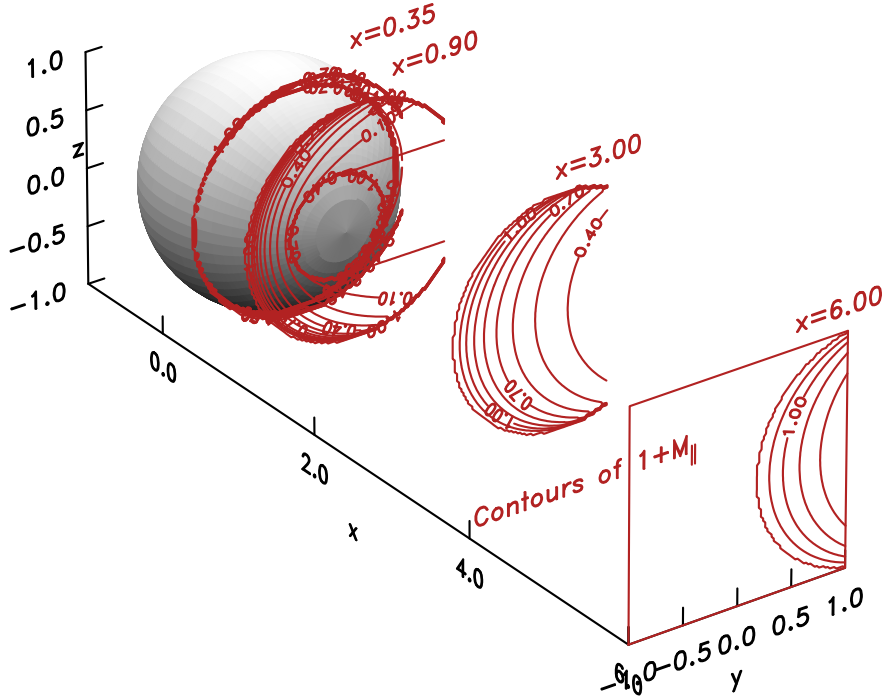to the surface, even if the surface-normal has a non-zero z-component. Therefore eq (15) is valid.

Figure 2: Contours of $M_\| + 1 = 1 + M_{\|\infty} + \ln(n/n_\infty)$ at intervals of 0.1, in planes of constant-x near a sphere of unit radius in a plasma with external drift velocity $M_{\|\infty} = 0.2$, $M_h = 0.24$.

As an illustration of this complete solution of the problem, Fig 2 shows a representation of the 3-Dimensional variation of $M_\|$ and equivalently $\ln n$ by contours of the quantity $M_\|+1$ drawn in perpendicular planes at various distances from a spherical object. Regions empty of contours to lower-y (left) of the contours shown have uniform unperturbed plasma. To the right of the contours is the wake region where the equations are not valid.

A second illustration is in Fig 3, which shows the contours for a pyramid shaped probe similar to what is used in Alcator C-Mod experiments[21]. A different drift velocity is illustrated.

3.2   Inclusion of external ∇n diamagnetic drift

The presence of a diamagnetic drift arising from external density gradient leads to several complicating factors. We consider an unperturbed density, n_∞, that in this case is not uniform but is a function also of perpendicular position. The usual case has $\nabla_\perp \phi_\infty$ and $\nabla_\perp n_\infty$ approximately parallel to each other, because both are perpendicular to the flux surface in a confined plasma. This is actually essential for the consistency of the unperturbed state, if it has no parallel gradients. Then the total drift velocity does not satisfy $\nabla.(n_\infty \mathbf{v}_\infty) = 0$
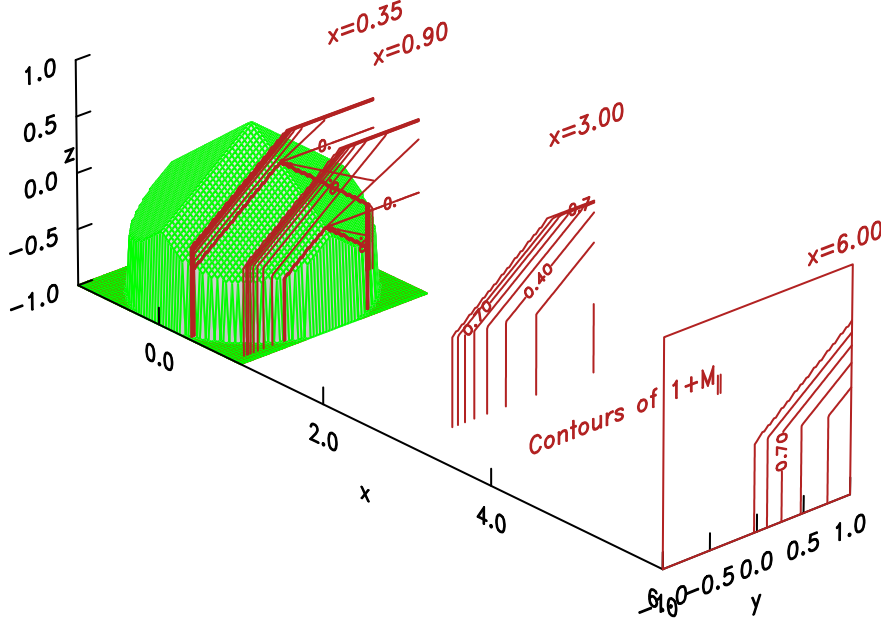
Figure 3: Contours of $M_\parallel + 1 = 1 + M_{\parallel\infty} + \ln(n/n_\infty)$ at intervals of 0.1, in planes of constant-x near a pyramidal Mach probe in a plasma with external drift velocity $M_{\parallel\infty} = -0.1$, $M_h = 0.15$.

unless $\mathbf{B}.(\nabla\phi_\infty \wedge \nabla n_\infty) = 0$ so that the drifts arising from the ϕ and n gradients are parallel to each other. We stick to this case here, and consistently take all external gradients to be in the z-direction, but note that effects in tokamak scrape-off-layers where parallel gradients are present and give rise to cross-flux-surface drifts are thereby ignored. In other words, we are dealing with a case of negligible parallel gradients in the external plasma.

We suppose that the external logarithmic gradient of the density is constant:

$$\nabla \ln n_\infty(z) = \hat{\mathbf{z}}/L_n, \tag{20}$$

where L_n is the (constant) density scale length. Equations (16) and (17) still apply. We still can rely upon integration along the negative characteristic to write down a relationship between n and $M_\parallel$, but that relationship is now

$$\ln n - M_\parallel = \ln(n_\infty(z_\infty)) - M_{\parallel\infty}, \tag{21}$$

where $n_\infty(z_\infty)$ is the unperturbed value of density at large distance from the probe, but at a value, z_∞, of z corresponding to tracking backward along the negative characteristic from the point of interest. Because n_∞ is a function of z when there are diamagnetic drifts, the value of $\ln n_\infty(z_\infty)$ depends upon the total z-displacement, $\delta z = z - z_\infty$ between the characteristic's start and the point of interest. Thus it is no longer the case that $n = n(M_\parallel)$.

Write the relationship between density and $M_\parallel$, deduced from the negative characteristic integration as

$$\ln(n/n_\infty(z)) = -M_{\parallel\infty} + M_\parallel - \delta z/L_n. \tag{22}$$

10

In this expression, δz is not a constant. We will demonstrate in the following, however, that a solution exists in which δz is a function only of $M_\parallel$. So taking $\delta z = \delta z(M_\parallel)$ we observe that $\ln(n/n_\infty)$ is also a function only of $M_\parallel$. [Here and following we use the notation n_∞ without an argument to denote the unperturbed density at the position of the point, $n_\infty(z)$ not $n_\infty(z_\infty)$.] The drift velocity from eq (17) can be written

$$
\mathbf{v}_\perp = - \left[\nabla \left(\phi_\infty + \frac{T_i}{Ze} \ln n_\infty \right) + \frac{mc_s^2}{Ze} \nabla \ln(n/n_\infty) \right] \wedge \frac{\mathbf{B}}{B^2} , \tag{23}
$$

in which the first two terms give rise to perpendicular Mach number $M_h = M_E + M_{ni}$, the sum of external $E \wedge B$ and ion diamagnetic drifts. The final term, which we identify as $\mathbf{M}_{\perp 1}$ is perpendicular to $\nabla \ln n/n_\infty$ and, because $\ln n/n_\infty$ is a function of $M_\parallel$, perpendicular also to $\nabla M_\parallel$.

Now we write the positive characteristic equation so as to use these expressions:

$$
\begin{aligned}
0 &= \left. \frac{d}{c_s dt} \right|_+ \left(\ln n + M_\parallel \right) = \left. \frac{d}{c_s dt} \right|_+ \left(\ln n/n_\infty + M_\parallel \right) + M_z/L_n \\
&= M_z/L_n + \left. \frac{d}{c_s dt} \right|_+ \left(2M_\parallel - \delta z/L_n \right) = M_z/L_n + \left. \frac{d}{c_s dt} \right|_+ \left(2 \ln n/n_\infty + \delta z/L_n \right), \tag{24}
\end{aligned}
$$

where we use the notation

$$
\left. \frac{d}{c_s dt} \right|_\pm \equiv \mathbf{M}.\nabla \pm \nabla_\parallel = (M_\parallel \pm 1) \frac{\partial}{\partial x} + M_y \frac{\partial}{\partial y} + M_z \frac{\partial}{\partial z} \tag{25}
$$

for the derivative along the positive or negative characteristics. Because the arguments of the derivatives in the last two forms of eq (24) are explicitly functions only of $M_\parallel$, we can subtract $\mathbf{M}_{\perp 1}.\nabla$ from the characteristic derivative without effect. In other words, in those expressions, we can interpret the derivative in the alternative version (valid only when operating on functions only of $M_\parallel$)

$$
\left. \frac{d}{c_s dt} \right|_\pm = (M_\parallel \pm 1) \frac{\partial}{\partial x} + M_h \frac{\partial}{\partial y} \tag{26}
$$

Now we eliminate y-derivatives of $\ln n$ from the last form of the positive characteristic equation using the expression for the z drift velocity:

$$
M_z = \rho_s \frac{\partial \ln n}{\partial y} = \rho_s \frac{\partial \ln n/n_\infty}{\partial y} \tag{27}
$$

to find

$$
(M_\parallel + 1) \frac{\partial}{\partial x} \ln n/n_\infty = -M_z \left(\frac{1}{2L_n} + \frac{M_h}{\rho_s} \right) - \frac{1}{2} \left. \frac{d}{c_s dt} \right|_+ \frac{\delta z}{L_n}. \tag{28}
$$

11

In the same way, we express the negative characteristic equation in terms of $\ln n/n_\infty$, reinterpret the derivative as the form (26) and then we eliminate x- and y-derivatives of $\ln n/n_\infty$ using eqs (28) and (27).

$$\frac{d}{c_s dt}\bigg|_- M_\parallel = \frac{d}{c_s dt}\bigg|_- \ln n/n_\infty + M_z/L_n$$

$$= \frac{M_\parallel - 1}{M_\parallel + 1}\left[-M_z\left(\frac{1}{2L_n} + \frac{M_h}{\rho_s}\right) - \frac{d}{c_s dt}\bigg|_+ \frac{\delta z}{2L_n}\right] + \frac{M_h M_z}{\rho_s} + \frac{M_z}{L_n}. \quad (29)$$

For compactness we define $d/dM_\parallel(\delta z/2L_n) \equiv r$; so that

$$\frac{d}{c_s dt}\bigg|_+ \frac{\delta z}{2L_n} = \frac{d}{c_s dt}\bigg|_+ M_\parallel \cdot \frac{d}{dM_\parallel}\frac{\delta z}{2L_n} = r\frac{d}{c_s dt}\bigg|_+ M_\parallel. \quad (30)$$

Eliminate $\frac{d}{c_s dt}\big|_+ M_\parallel$ between this expression and the $M_\parallel$ form of eq (24) to obtain

$$\frac{d}{c_s dt}\bigg|_+ \frac{\delta z}{2L_n} = -\frac{M_z}{2L_n}\frac{r}{1-r}. \quad (31)$$

Substituting into eq (29) and eliminating M_z and the right hand side's $\frac{d}{c_s dt}\big|_- M_\parallel$ using the identity

$$r = \frac{d}{c_s dt}\bigg|_- \frac{\delta z}{2L_n}\bigg/ \frac{d}{c_s dt}\bigg|_- M_\parallel = \frac{M_z}{2L_n}\bigg/ \frac{d}{c_s dt}\bigg|_- M_\parallel , \quad (32)$$

we arrive at the following quadratic equation for r

$$1 = \frac{r}{M_\parallel + 1}\left[M_\parallel + 3 + \frac{r}{1-r}(M_\parallel - 1) + 4L_n M_h/\rho_s\right]. \quad (33)$$

We solve this equation, using the simplifying notation

$$u_0 \equiv 2L_n M_h/\rho_s , \qquad u \equiv M_\parallel + u_0 , \quad (34)$$

to find

$$r = (1/4)[u + 2 \pm \sqrt{u^2 + 4u_0}] . \quad (35)$$

Then we can integrate to obtain the z-displacement

$$\frac{\delta z}{L_n} = 2\int r\, dM_\parallel = \frac{1}{4}\left[u^2 + 4u \mp \left\{u\sqrt{u^2 + 4u_0} + 4|u_0|\ln\left(\pm u + \sqrt{u^2 + 4u_0}\right)\right\}/2\right]_{u_\infty}^u , \quad (36)$$

where the upper or lower sign is to be chosen when u_0 is positive or negative respectively. This solution is real only if $1/u_o > -1/4$, which is equivalent to the requirement that the ion diamagnetic drift magnitude $|M_{ni}|$ be less than the $E \wedge B$ drift magnitude $|M_E|$. Positive u_0 corresponds to M_{ni} in the opposite direction to M_E. For negative u_o the two drifts have the same polarity.
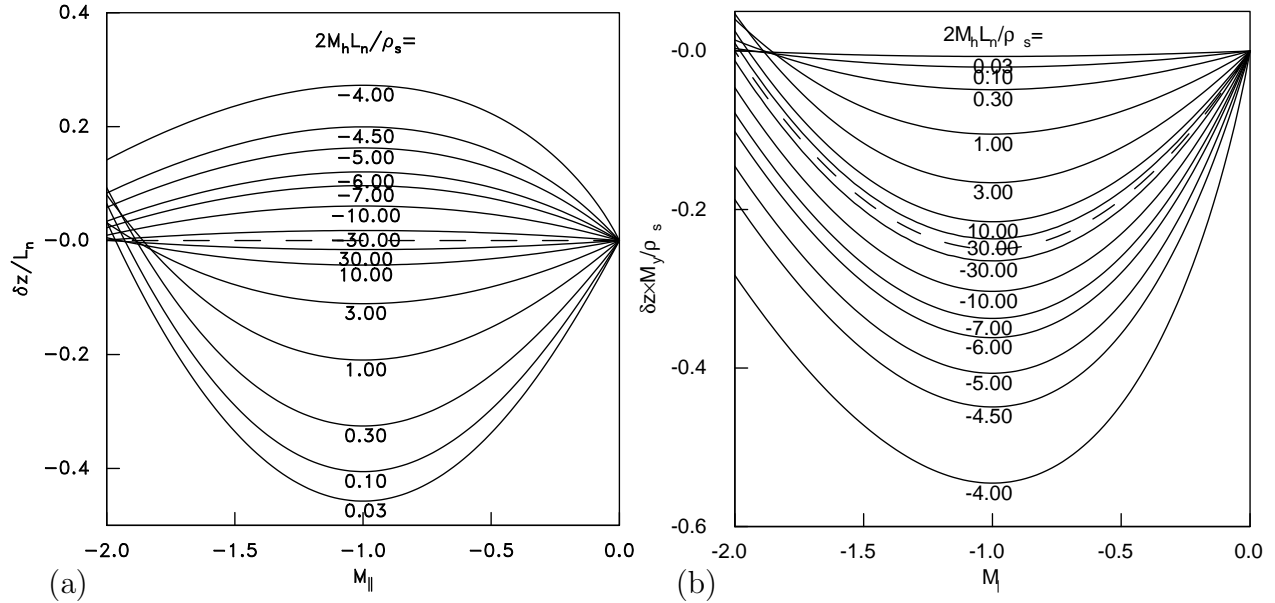
Figure 4: Solutions for the z-displacement normalized to the density scale-length (a) or the Larmor radius (b), for the full allowed range of $u_0 = 2M_h L_n/\rho_s$. It is assumed that $M_{\parallel\infty}$ is zero, but the curve shapes are the same regardless of the starting value of $M_{\parallel}$.

In Fig 4 are plotted the solutions for δz as a function of $M_{\parallel}$ for the full range of allowable u_0. Whether normalized by L_n or by ρ/M_h, these results show that the displacement, while substantial, is bounded. Moreover the curves are quite close to being mirror-symmetric about the line $M_{\parallel} = -1$.

The value of δz together with the negative characteristic integration, eq (22) provide the complete solution for $\ln(n/n_\infty)$ which is a function only of $M_{\parallel}$. The characteristic equations can be considered to be

$$\frac{d}{c_s dt}\bigg|_{\pm} (\ln n/n_\infty \pm M_{\parallel}) = \frac{M_z}{L_n}, \tag{37}$$

in which the characteristic derivatives can be taken as eq (26), that is, lying in a $z = const$ plane. The characteristics are now curved, and cannot be constructed directly from the geometry, as was possible in the absence of diamagnetic drift. But this does not matter for the purposes of obtaining the flux to the probe. The boundary condition at the plasma edge is, as before, that provided the boundary is convex, the positive characteristic must be tangential to the surface; that is, $M_{\parallel} + 1 = M_h \cot\theta$.

In practice, the perpendicular velocity is generally deduced from Mach probe measurements effectively by comparing values of the ion current density for faces having equal and opposite values of $\cos\theta$; that is, having the same angle to the magnetic field, but pointing upstream or downstream with respect to the perpendicular flow. Although δz changes the value of $\ln n$ and thus affects the ion flux density, if δz is of exactly even parity in $M_{\parallel} + 1$ and hence in $\cot\theta$, it will contribute nothing to the ratio of the ion fluxes on which the
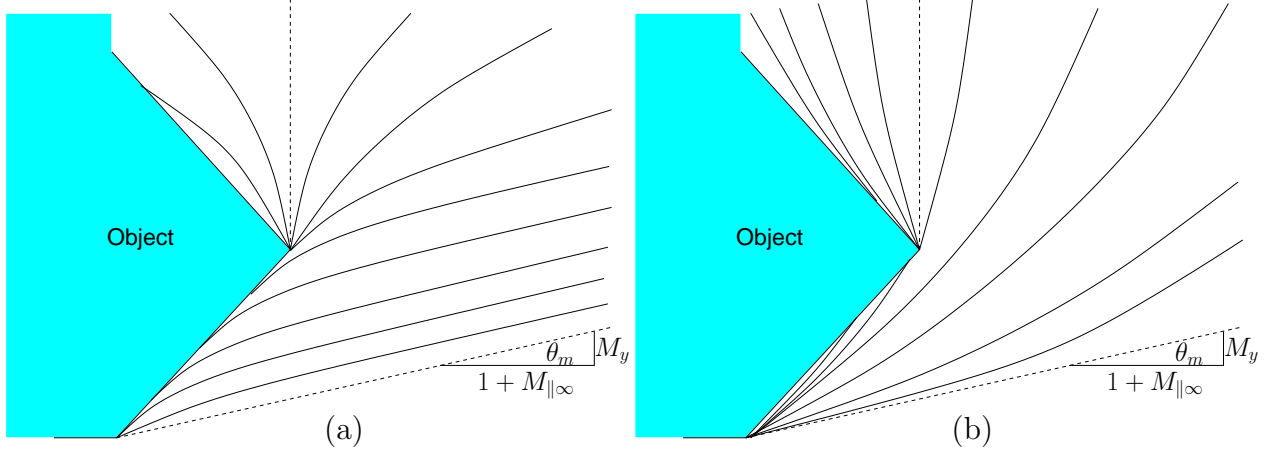
13

Figure 5: Schematic illustration of shape of positive characterstics in the x-y plane. In (a) L_n is positive corresponding to diamagnetic drift opposing $E \wedge B$ drift, and the displacement δ_l being down the density gradient. In (b) L_n is negative.

measurement is based. For $L_n \to \infty$ (zero diamagnetic drift) and $M_h L_n = 0$ (zero net drift) δz is indeed exactly of even parity. The maximum value of the odd-parity part of $\delta z / L_n$ is approximately 0.02 for $|M_\parallel + 1| < 0.6$ for all u_0 (and for $u_0 = 2 M_y L_n / \rho_s > 3$ it is considerably smaller). Thus the contribution of the δz term to Mach probe velocity measurement is typically less than 2%, which is for practical purposes negligible. The magnitude of δz is sufficiently great, however, that it would be inadvisable to attempt to deduce the perpendicular flow without taking advantage of its approximate parity. In other words, a Mach-probe measurement really must be based on electrodes with equal and opposite values of $\cot \theta$, and not, for example, on comparing positive $\cot \theta$ with $\cot \theta = 0$.

It is, in effect, the δz variation that causes the positive characteristics to have curvature. This curvature has magnitude approximately $1/L_n$. When considering whether or not a probe surface is convex, this curvature has to be accounted for. Schematic representations of the positive characteristic shapes are illustrated in Fig 5, for an object with two plane faces. When the curvature is towards such a face, it is concave, and the plasma flows into the probe with a negative parallel velocity greater than $1 - M_y \cot \theta$. This concavity is avoided in general if the probe has a convex curvature that is greater than $1/L_n$. The characteristics curve either away from or towards the line $x = const.$ depending on whether L_n is positive or negative. (M_y is taken always positive.)

To summarize, then, the ion flux per unit perpendicular area from the plasma to a convex surface in the presence of combined (colinear) $E \wedge B$ and density-gradient diamagnetic external drifts can be written precisely as eq (15):

$$\Gamma_\parallel = n c_s = n_\infty(z_\infty) c_s \exp[-1 - (M_{\parallel\infty} - M_h \cot \theta)], \tag{38}$$

but with

$$M_h = M_E + M_{ni} \tag{39}$$

14

and

$$n_\infty(z_\infty) = n_\infty(z - \delta z) = n_\infty(z) \exp(-\delta z/L_n). \tag{40}$$

Because of its near even parity in $M_\parallel + 1$, the δz term can generally be ignored for the purposes of $M_\perp$ determination.

4 Effects from presheath displacement

The expressions obtained so far are for the flux leaving the plasma region where the drift expressions hold. Between that region and the probe surface lie the magnetic presheath, of order a Larmor radius thick, which we assume is small compared with the probe, and the Debye sheath, of order 4 Debye lengths thick, which we shall ignore altogether. The dynamics in the magnetic presheath are not ignorable. The flux to the probe itself is different from the flux from the plasma into the magnetic presheath when diamagnetic drifts are important.

4.1 Magnetic presheath displacement calculation

In the magnetic presheath, the electric field normal to the surface is strong enough that $E_\perp/B$ is of order the sound speed. The normal gradients of the resulting drift give rise to non-negligible convective derivative (i.e. polarization drift) terms. Indeed, it is those terms that permit the ion fluid trajectory to acquire sufficient cross-field velocity to satisfy the Bohm condition at the Debye-sheath edge. We assume on the magnetic presheath scale the probe surface can be approximated as planar and the gradients can be considered all to be normal to it. Let the direction of the normal (outward from the plasma) to the probe surface be $\hat{\mathbf{k}}$. Define $\sin\alpha = -\hat{\mathbf{k}}.\mathbf{B}/B$ and the unit vector $\hat{\mathbf{l}} = \mathbf{B} \wedge \hat{\mathbf{k}}/B\cos\alpha$ in the direction perpendicular to $\mathbf{B}$ and $\hat{\mathbf{k}}$. Define the third unit vector by $\hat{\mathbf{j}} = \hat{\mathbf{k}} \wedge \hat{\mathbf{l}}$. See figure 6. Denote vector components in the respective directions by subscripts. Then the (normal) $\hat{\mathbf{k}}$-component of the momentum equation (2) is

$$m\mathbf{v}.\nabla v_k = -Ze\nabla_k\phi - (1/n)\nabla_k p + Ze\mathbf{v}.(\mathbf{B} \wedge \hat{\mathbf{k}}) \tag{41}$$

we eliminate the potential gradient using eq (16), and density gradient using the continuity equation (1) in the form $nv_k = const.$, so that $\nabla_k \ln n = -\nabla_k \ln v_k$, to obtain

$$v_l\Omega_i \cos\alpha = (-c_s^2/v_k + v_k)\nabla_k v_k . \tag{42}$$

We wish to calculate the total displacement, δ_l in the $\hat{\mathbf{l}}$-direction, experienced by the ion fluid traversing the magnetic presheath. This is simply the time integral of eq (42):

$$\delta_l\Omega_i \cos\alpha = \int(-c_s^2/v_k + v_k)\nabla_k v_k dt = \int(1 - c_s^2/v_k^2)dv_k = [v_k + c_s^2/v_k] , \tag{43}$$

(recognizing that $v_k dv_k/dx_k = dv_k/dt$). The limits of the integral are $v_k/c_s = \Gamma_k/nc_s \equiv S$ at the magnetic presheath outer edge (where Γ_k is the normal flux density) and $v_k/c_s = 1$ at its inner edge, entering the Debye sheath (whose thickness we ignore). Therefore

$$\delta_l = \rho_s[2 - S - 1/S]/\cos\alpha = -\rho_s\frac{[1 - S]^2}{S\cos\alpha} . \tag{44}$$
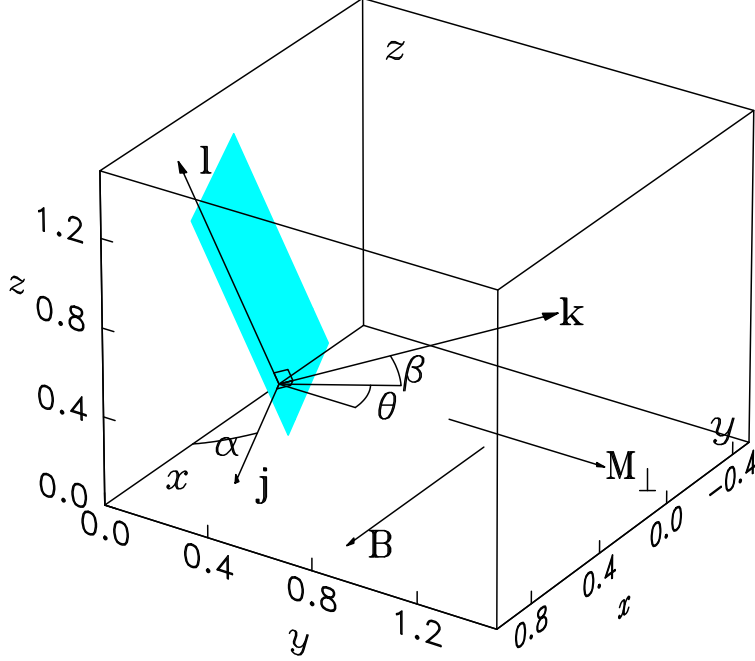
Figure 6: Illustration of the coordinates referred to the field and drift directions (x, y, z) and the unit vectors referred to the probe surface directions $(\hat{\mathbf{j}}, \hat{\mathbf{k}}, \hat{\mathbf{l}})$.

Thus, for small incidence angle of the magnetic field (S small) a rather large displacement ($\delta_l \sim \rho_s/S$) along the magnetic presheath occurs. This displacement has been noted and roughly estimated [18] in previous discussions of magnetic presheath structure. Its significance is that ions exit the magnetic presheath (and are collected by the probe) a tangential distance δ_l from where they entered it. If there is a tangential gradient $\nabla_l\Gamma_k$ of the normal flux-density Γ_k entering the magnetic presheath at position x_l, then the flux-density to the probe will be not $\Gamma_k(x_l)$ but $\Gamma_k(x_l - \delta_l) = \Gamma_k(x_l)\exp[-\delta_l\nabla_l\ln(\Gamma_k)]$ (choosing consistently with our $\ln n$ assumption, uniformity of $\nabla\ln\Gamma_k$ when surface curvature is ignored). This alteration of the flux-density is precisely the phenomenon that Cohen and Ryutov [19] calculated in the small-α limit. In their Eulerian viewpoint, the alteration is attributable to divergence of the tangential flux in the magnetic presheath. From the present Lagrangean viewpoint, it arises from the integrated convective derivative. We can demonstrate this by evaluation. Identifying $\nabla\ln\Gamma_k = \nabla\ln n_\infty$ and using the definitions of S and $\hat{\mathbf{l}}$ we find

$$
\begin{aligned}
\delta_l\nabla_l\ln\Gamma_k &= -\frac{[1-S]^2}{S\cos\alpha}\rho_s\hat{\mathbf{l}}.\nabla\ln\Gamma_k = -\frac{[1-S]^2}{S\cos^2\alpha\,c_s}\frac{T_i + ZT_e}{ZeB^2}(\nabla\ln n_\infty \wedge \mathbf{B}).\hat{\mathbf{k}} \\
&= \frac{[1-S]^2}{S\cos^2\alpha\,c_s}(\mathbf{v}_{ni} - \mathbf{v}_{ne}).\hat{\mathbf{k}} = \frac{[1-S]^2\hat{k}_y}{S\cos^2\alpha}(M_{ni} - M_{ne})
\end{aligned}
\tag{45}
$$

Cohen and Ryutov's calculation assuming small S and α gave this expression with the geometric term $[1-S]^2\hat{k}_y/\cos^2\alpha$ equal to 1, yielding a $\delta_l\nabla_l\Gamma_k$ equal to the difference between the ion and electron diamagnetic normal flux densities. Now we evaluate the total flux

16

density to the probe using eq (38), which yields $S = \sin\alpha$, and recognizing that when the orientation of $\hat{\mathbf{k}}$ perpendicular to B is defined by setting $\hat{k}_z = \sin\beta$, it immediately follows that $\hat{k}_x = -\cos\beta\sin\theta$, $\hat{k}_y = \cos\beta\cos\theta$ and $\sin\alpha = \cos\beta\sin\theta$. We obtain

$$\Gamma_k(x_l - \delta_l) = nc_s \sin\alpha \exp\left\{-\left[\frac{1-\sin\alpha}{1+\sin\alpha}\right](M_{ni} - M_{ne})\cot\theta\right\} . \tag{46}$$

The ion flux to the probe surface per unit perpendicular area is then

$$\Gamma_{\|p} = n_\infty c_s \exp\left\{-1 - M_{\|\infty} + M_h \cot\theta - \left[\frac{1-\sin\alpha}{1+\sin\alpha}\right](M_{ni} - M_{ne})\cot\theta\right\} . \tag{47}$$

The logarithm of ratio of the flux for positive and negative $\cos\theta$ is

$$\ln(\Gamma_+/\Gamma_-) = -\frac{\delta z_+ - \delta z_-}{L_n} + 2M_h\cot\theta - 2\frac{1-\sin\alpha}{1+\sin\alpha}(M_{ni} - M_{ne})\cot\theta . \tag{48}$$

Ignoring the δz term, this becomes

$$\frac{\ln(\Gamma_+/\Gamma_-)}{2\cot\theta} = M_E + \frac{M_{ni}2\sin\alpha + M_{ne}(1-\sin\alpha)}{1+\sin\alpha}. \tag{49}$$

Thus, in addition to M_E, the velocity combination measured by the Mach probe ratio is an interpolation between the ion and electron diamagnetic velocities (which of course have opposite sign), dependent upon the angle α between the probe face and the field. Normally in practice an intermediate value of θ (not too small but not too close to $\pi/2$) must be used, which generally means an intermediate value of α.

4.2   Probe curvature and finite facet size

The displacement in the magnetic presheath also gives rise to a flux correction when the probe surface has curvature. The flux at any point on an electrode is characteristic of the flux into the magnetic presheath at a position $-\delta_l$ away. If the surface is curved, then the *angles* at that position will be different, giving rise to a different flux. But also, the displacement may have a divergence, which gives rise to flux enhancement even if the flux into the magnetic presheath were uniform.

We note that the displacement strictly contains a component δ_j, along the direction $\hat{\mathbf{j}} \equiv \hat{\mathbf{k}} \wedge \hat{\mathbf{l}}$, which for small α is mostly along $\mathbf{B}$, and is of approximate magnitude $\rho_s/\sin\alpha$, similar to δ_l. This displacement δ_j can be calculated in the form of a closed integral expression by solving the magnetic presheath equations using the techniques of references [22, 4]. We ignore it, here and in the previous section, because it is mostly motion along the magnetic field, which can be considered to be accounted for by surface projection along the field, and because both the projection and any additional cross-field motion (in the $\hat{\mathbf{k}}$-direction) that makes δ_j different from the pure field-line projection, make flux contributions that are symmetric: of even parity under reversals of k_y and hence of $\cos\theta$. In other words, there is a small correction to the total flux density from δ_j, which can be pictured as arising

17

from the fact that the probe collects ions from a cross-field area that is larger than its solid cross-section by a margin of width approximately ρ_s. But that correction does not affect the deduced Mach-numbers, because they are based on ratios of collection fluxes from surfaces with opposite k_y, which are equally perturbed by even-parity terms.

The perpendicular flux-density perturbation arising from δ_l along $\hat{\mathbf{l}}$ has contributions $\delta_l \partial n / \partial x_l = \delta_l n M_h \partial \cot\theta / \partial x_l$ and from the convective derivative of the perpendicular area element, which can be written (differentially) $\Delta A / A = \nabla^s(\delta_l \hat{\mathbf{l}}) = \delta_l \nabla^s.\hat{\mathbf{l}} + \hat{\mathbf{l}}.\nabla^s \delta_l$, where ∇^s denotes the two-dimensional gradient $(\partial/\partial y, \partial/\partial z)$ in the perpendicular coordinates, but evaluated along the probe surface (not at constant x). Thus the total correction arising from surface curvature is

$$ -\Delta\Gamma_\| / \Gamma_\| = M_h \delta_l \hat{\mathbf{l}}.\nabla^s \cot\theta + \delta_l \nabla^s.\hat{\mathbf{l}} + \hat{\mathbf{l}}.\nabla^s \delta_l \ . \tag{50} $$

In this equation the first term has even parity with respect to k_y-reversal and therefore does not contribute to flow-measurement bias. The last two have odd parity and do contribute. Their order of magnitude is δ_l / R_c where R_c is the typical radius of curvature of the surface. (Note that this is a real physical effect, not the elementary mathematical integration discussed by Pelemann et al[23].)
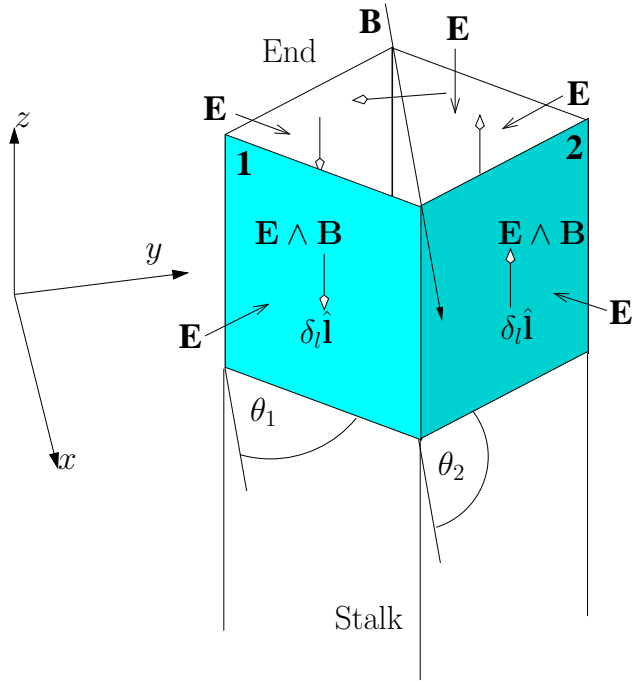

Figure 7: Illustration of the opposite directions of magnetic presheath displacement $(\delta_l \hat{\mathbf{l}})$ for opposite values of $\cos\theta$. The electric field is towards the probe and $\delta_l \hat{\mathbf{l}}$ is in the $\mathbf{E} \wedge \mathbf{B}$ direction. When the displacement is towards the stalk, as it is for facet 1 but not facet 2, a depleted region exists at the probe end. (In this figure "forward" is up and "backward" is down.)

A related, but more intuitive and probably more relevant correction comes from edges of plane facets. Most Mach probes have electrodes at or near their ends [12, 9, 13, 24] The direction $\delta_l \hat{\mathbf{l}}$ associated with the surfaces points forward, beyond the probe end, on one side and backward towards the probe stalk on the other, as illustrated in Fig 7. The surface for which it points backward collects essentially zero flux for a distance $\approx \delta_l$ from the end, because of the magnetic presheath displacement; then it collects the full flux from then on. The surface for which $\delta_l \hat{\mathbf{l}}$ points forward collects full flux at its end. The electrode will collect full flux throughout its area, provided that it is embedded in a surface of constant angle which extends a distance $\approx \delta_l$ past the (backward) edge of the electrode. Therefore the likely effect (dependent on the detailed electrode placement) of δ_l is to induce a depleted flux region on *just the forward edge* of *just the electrode for which $\delta_l \hat{\mathbf{l}}$ is backward*. An appropriate estimate of the odd-parity part of the resulting flux change is

$$\Delta\Gamma_\parallel/\Gamma_\parallel \approx \delta_l \hat{l}_z/2\bar{h} = -\frac{\rho_s(1-S)^2\cos\beta}{2\bar{h}S\cos\alpha} \approx -\rho_s\frac{(1-\sin\alpha)^2}{2\bar{h}\cos\alpha\sin\theta} \ , \tag{51}$$

approximating S as $\sin\alpha$ to lowest order in $M_\perp$, and denoting the average z-extent of the electrode as $\bar{h}$.

Since in a perpendicular Mach-probe measurement M_h is estimated from the expression

$$M_h|\cot\theta| = (1/2)\ln[\Gamma_{\parallel+}/\Gamma_{\parallel-}] \ , \tag{52}$$

(where subscript $\pm$ refers to the sign of $\cos\theta$) the perturbation ΔM_h to the deduced M_h is related to the odd-parity perturbation to flux, $\Delta\Gamma_\parallel$, by

$$\Delta M_h = |\tan\theta|\Delta\Gamma_\parallel/\Gamma_\parallel \approx -\frac{\rho_s}{2\bar{h}}\frac{(1-\sin\alpha)^2}{\cos\alpha\cos\theta} \ . \tag{53}$$

There is therefore an intrinsic bias of order $\rho_s/2\bar{h}$ in such a Mach-probe measurement. Its direction is such that if the gradient of plasma pressure is in the forward direction of the probe, in other words the probe is introduced from the "outside" of the plasma where pressure is low (as is generally the case), then the spurious apparent drift is in the same direction as the ion-diamagnetic drift. This end-effect can in principle be avoided if the electrode does not sample the plasma at the end of the facets, but instead approaches the end no closer than a z-distance of approximately $\rho_s(1-S)^2\cos\beta/(S\cos\alpha)$.

5   Temperature gradient drifts

Diamagnetic drifts might also arise from temperature gradients, which have so far been excluded. A physically justifiable approach for electron temperature gradients simply regards T_e as constant along the field, but having an externally imposed gradient in the z-direction. A similar mathematical ansatz will be applied to T_i but with less clear physical justification. The equations of continuity and parallel momentum (6) are unchanged by allowing

z-variation of temperature. However, when they are rearranged into characteristic form one obtains

$$(\mathbf{v}.\nabla \pm c_s\nabla)[\ln n/n_\infty \pm v_\parallel/c_s] = \pm v_\parallel(\mathbf{v}.\nabla_\perp)(1/c_s) \equiv \pm(v_\parallel/c_s)(-v_z/L_c) . \tag{54}$$

Here c_s is a function of z because of temperature gradients. Its gradient has been written as $dc_s/dz = c_s/L_c$. It gives rise to the inhomogeneous term on the RHS which is the same order as the LHS terms near the boundary of the unperturbed region. It cannot therefore simply be ignored because of ordering. However, its effects are to change the value of $\ln n/n_\infty - v_\parallel/c_s$ along the negative characteristic, which is what determines the flux at the boundary. This change can be calculated, and proves to be usually ignorable, as we now show. We assume that the value of this combination can be expressed as a function only of $M_\parallel$:

$$\ln n/n_\infty - M_\parallel = g(M_\parallel) \tag{55}$$

and solve for g using the same approach as we used for density gradients. To keep the algebra in check we assume *no* external density gradients for this calculation. Initially we consider only the c_s-variation. In outline, the calculation is as follows.

The positive characteristic equation gives

$$- M_\parallel v_z/L_c = \left.\frac{d}{dt}\right|_+ (2M_\parallel + g) = \left.\frac{d}{dt}\right|_+ (2\ln n/n_\infty - g) \tag{56}$$

We define $dg/dM_\parallel = 2q$ so that $\left.\frac{d}{dt}\right|_\pm g = 2q\left.\frac{d}{dt}\right|_\pm M_\parallel$ and eliminate $M_\parallel$ derivatives from the characteristics to obtain

$$\left.\frac{d}{dt}\right|_- g = -M_\parallel\left(\frac{-v_z}{L_c}\right) \quad , \quad \left.\frac{d}{dt}\right|_+ g = M_\parallel\left(\frac{-v_z}{L_c}\right)\frac{q}{1+q}. \tag{57}$$

We eliminate partial x-derivatives of $\ln n/n_\infty$ between the positive and negative characteristics, and partial y-derivatives using the z-velocity expression (27). Substituting for the characteristic derivatives of g and dividing the resultant through by $(-v_z/2L_c)$ we arrive at

$$\frac{M_\parallel - 1}{M_\parallel + 1}\left[M_\parallel\frac{q}{1+q} + \frac{2v_h L_c}{\rho_s} + M_\parallel\right] - \frac{2v_h L_c}{c_s\rho_s} + M_\parallel\left(2 + \frac{1}{q}\right) = 0 . \tag{58}$$

This quadratic equation for q can be solved to obtain

$$\frac{1}{2}\frac{dg}{dM_\parallel} = q = \frac{-(2M_\parallel^2 + M_\parallel - u_1) \pm \sqrt{(1 - 2u_1)M_\parallel^2 + u_1 M_\parallel + u_1^2}}{4M_\parallel^2 - 2u_1} \tag{59}$$

where $u_1 \equiv 2v_h L_c/c_s\rho_s$.

Provided $M_{\parallel\infty}$ and u_1 are indeed constant, this is a consistent solution. In view of the variation of c_s and hence ρ_s with z, it is clear that the constancy of u_1 requires $c_s(z)$ to satisfy a simple differential equation, whose solution gives the required $c_s(z)$. This is not as
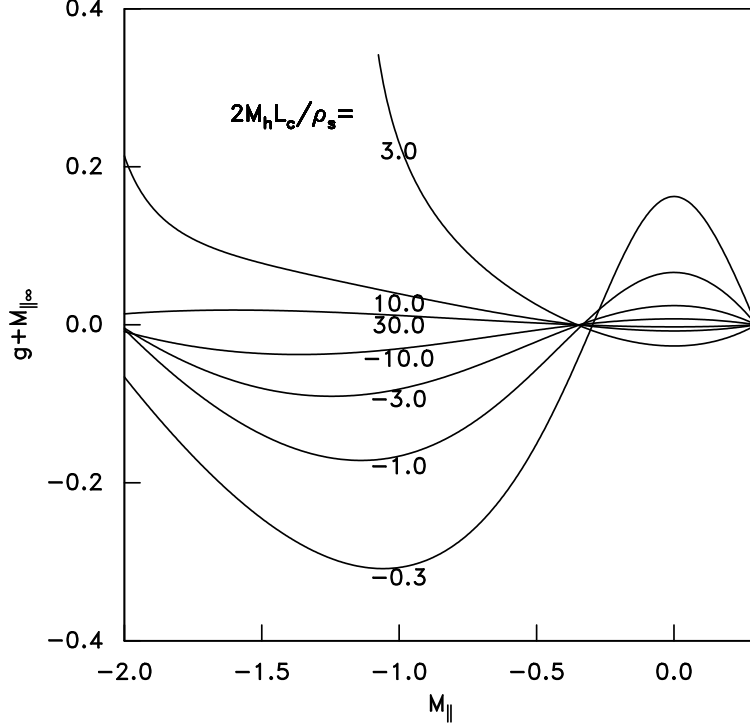
Figure 8: Solutions for the quantity $g + M_{\|\infty} = \ln n/n_\infty - M_\| + M_{\|\infty}$ accounting for perpendicular gradients of sound-speed when external temperature gradients contribute to the drift.

simple a profile as the linear $\ln n_\infty$ profile for the density-gradient. But we are interested in a local region on the gradient, where it is acceptable to choose the precise form of $c_s(z)$ to satisfy the consistency condition without substantially changing the problem, in-so-far as a local expansion of c_s is allowable.

Equation (59) can be integrated analytically, but the resulting expression would be extremely long and cumbersome, so it is not given here. Instead, numerical integrations are illustrated in Fig 8. The case $M_{\|\infty} = 0.2$ is shown, to emphasize the applicability of the solution shapes to all $M_{\|\infty}$. The solution becomes imaginary for some relevant negative values of $M_\|$ when $0 < u_1 \lesssim 10$, illustrated by the $u_1 = 3$ curve. Provided such parameters are avoided, it can be seen that the values and especially the odd parity (in $M_\| + 1$) part of $g + M_{\|\infty}$ are small.

A second modification of the governing equations, arising from temperature gradients, is that additional terms are present in the drift velocity eq (3). Ion temperature gradients are easy to treat because they can be expressed as a uniform term like $\nabla\phi_\infty$, but T_e gradients introduce a new type of term (c.f. 23). The total drift velocity is:

$$\mathbf{v}_\perp = - \left[\ln(n/n_\infty)\nabla\left(\frac{T_e}{e}\right) + \nabla\left(\phi_\infty + \frac{T_i}{Ze}\right) + \frac{T_i}{Ze}\nabla\ln n_\infty + \frac{mc_s^2}{Ze}\nabla\ln n/n_\infty \right] \wedge \frac{\mathbf{B}}{B^2} . \quad (60)$$

We can still discard the final ($\nabla\ln n/n_\infty$) term as an $\mathbf{M}_{\perp 1}$ giving no advection because

21

$\mathbf{M}_{\perp 1}.\nabla \ln n/n_\infty = 0$. The rest should be regarded as v_h, having no z-component. The first term is the new one, so far not treated. It is non-uniform; but a function of $\ln n/n_\infty$ and hence, within the solution schemes we have developed, a function of $M_\parallel$. The v_h variation can be incorporated into the scheme above, except that the consistency condition upon the c_s profile becomes that $u_1 = v_h 2L_c/c_s\rho_s$ which varies with v_h, must be a function only of $M_\parallel$. Assuming an appropriate c_s shape is chosen, eq (59) still applies, and could still be integrated provided that $u_1(M_\parallel)$ were known. Plainly, provided that u_1 stays within acceptable ranges during the integration, curves that bear resemblance to those of Fig (8) will be obtained. Generally then, the arguments that $g + M_{\parallel\infty}$ can usually be ignored will remain as valid as before, provided u_1 stays within the range of their validity.

The boundary condition at the plasma edge is still that the positive characteristic be tangent to the probe surface, that is (eq 14) $M_\parallel = M_h \cot\theta - 1$, but with the following definition:

$$\mathbf{M}_h = -\left[\ln(n/n_\infty)\nabla\left(\frac{T_e}{e}\right) + \nabla\left(\frac{T_i}{Ze} + \phi_\infty\right) + \frac{T_i}{Ze}\nabla\ln n_\infty\right]\wedge\frac{\mathbf{B}}{B^2 c_s} \qquad (61)$$

$$= -\ln(n/n_\infty)M_{Te} + M_{Ti} + M_E + M_{ni} , \qquad (62)$$

where M_{Te} and M_{Ti} are the (external) diamagnetic drift due to temperature gradient of the electrons and ions. We can then substitute into eq (55) to eliminate $M_\parallel$ and obtain after rearrangement:

$$\ln n/n_\infty = \frac{-1 + g + (M_{Ti} + M_E + M_{ni})\cot\theta}{1 + M_{Te}\cot\theta} , \qquad (63)$$

in which, for the purposes of perpendicular velocity measurement, we can take $g \approx -M_{\parallel\infty}$. To first order in the perpendicular velocities this can be written

$$\ln n/n_\infty \approx -1 - M_{\parallel\infty} + [(1 + M_{\parallel\infty})M_{Te} + M_{Ti} + M_E + M_{ni}]\cot\theta , \qquad (64)$$

showing that the effect of the electron temperature-gradient drift can be amplified or attenuated, compared with the other drifts, depending upon the parallel external velocity $M_{\parallel\infty}$.

Finally we must account for the temperature gradients in the correction arising from magnetic presheath displacement. We can ignore the next order corrections to δ_l arising from approximations in its derivation. But we must account for the fact that since $\delta_l \propto c_s$, a transverse derivative of c_s gives rise to transverse divergence which alters the flux density as it traverses the magnetic presheath. The change in area A arising from this effect is $\Delta A/A = \delta_l \hat{\mathbf{l}}.\nabla \ln c_s$. This gives rise to a change in $\ln\Gamma$ of $-\delta_l\hat{\mathbf{l}}.\nabla\ln c_s$. In addition, the displacement gives rise to a convective difference between the flux to the probe and that entering the presheath that, since $\Gamma \propto nc_s$ can be expressed as

$$\Delta\ln(nc_s) = -\delta_l\hat{\mathbf{l}}.(\nabla\ln n + \nabla\ln c_s) \qquad (65)$$

adding these two effects gives the total magnetic presheath difference:

$$\Delta\ln\Gamma_k = -\delta_l\hat{\mathbf{l}}.(\nabla\ln n + 2\nabla\ln c_s) = -\delta_l\hat{\mathbf{l}}.(\nabla\ln n + \nabla\ln(ZT_e + T_i)) \qquad (66)$$

Applying the transformations of eq (45), we see that our result is the same as before except that the total diamagnetic difference velocity $M_D \equiv M_{Di} - M_{De} = (M_{ni} + M_{Ti}) - (M_{ne} + M_{Te})$ is involved rather than just the density-gradient part calculated before.

The final expression for flux per unit perpendicular area to the probe is thus

$$\frac{\Gamma_{\|p}}{nc_s} = \exp\left\{\frac{-1 + g + (M_{Ti} + M_E + M_{ni})\cot\theta}{1 + M_{Te}\cot\theta} - \left[\frac{1 - \sin\alpha}{1 + \sin\alpha}\right](M_{Di} - M_{De})\cot\theta\right\}, \quad (67)$$

or, to first order in perpendicular velocities, and approximating g,

$$\ln\left\{\frac{\Gamma_{\|p}}{nc_s}\right\} = -1 - M_{\|\infty} + \left[(1 + M_{\|\infty})M_{Te} + M_{Di} + M_E - \left(\frac{1 - \sin\alpha}{1 + \sin\alpha}\right)M_D\right]\cot\theta, \quad (68)$$

where α is the angle between the probe surface and the magnetic field (in 3-dimensions), and θ is the angle within the plane containing field and external drift. All drift velocities here refer to the external, unperturbed plasma.

6   Discussion

The complete solution of the drift equations that has been obtained here is highly appropriate when the $E \wedge B$ drift dominates. Then the positive characteristics are straight and the full solution in the plasma region can readily be constructed. Notice that the parallel length of the presheath (i.e. the perturbed plasma region) is approximately the transverse size of the probe a (say) times $(M_\| + 1)/M_\perp$. If the perpendicular Mach number is not very small, this length $\sim a/M_\perp$ is likely substantially shorter than that from the standard diffusive estimate: $a^2 c_s/D$. Certainly it can easily be shorter than the mean-free-path for electron-ion Coulomb collisions, which is required for the ignoring of friction inherent in our treatment. In such a situation taking the electron temperature to be invariant along the field is completely natural. It is not so natural to make that approximation for the ions. However, it is known from other calculations [25, 9] that the isothermal approximation gives results quite close to those that arise from more physically plausible approximations. In any case, the standard widely-accepted formulas are based upon isothermal-ion calculations. In addition to providing rigorous analytical justification, regardless of probe geometry, for formulas that are practically the same as those arising from a diffusive treatment, the present treatment helps to resolve another conceptual problem of long standing. It is that probes are often smaller than the typical transverse size of the turbulence that is responsible for transport in the regions of plasma in which they are used. In other words, transport, for example in tokamak edges and scrape-off-layers, is actually known to be dominated by fluctuating cross-field flows that in many situations have eddies larger than the probes. In such situations, using a heuristic approximation that cross-field flux is expressible through a diffusion coefficient, as prior treatments have done, is questionable. The present treatment, regarded as a short-time snap-shot of a situation that is fluctuating, is more appropriate. Fortunately the result is the same, although with much sharper physical justification.

The drift-approximation is unproblematic for $E \wedge B$ drifts, because there is nothing to prevent the probe being bigger than the Larmor radius while the drift Mach number is of order unity. This is not so for diamagnetic drifts. The diamagnetic Mach number is of order $M_D \sim \rho_s/L$ (where L is the pressure scale-length). Consequently if $M_D \sim 1$, there is no separation of scales between the Larmor radius and the gradient scale-length. It is then impossible to choose a probe size that is both bigger than the Larmor radius (in order to justify the drift approximation) and smaller than the gradient scale-length (to justify a local approximation of the drifts). This is an inherent difficulty that underlies the need in the calculations to choose a specific shape of the plasma profiles. Only if M_D is small does a local approximation to the flow make sense. Therefore, the usefulness of the present calculation is increasingly compromised as M_D approaches unity. A calculation that avoids the drift-approximation is then really needed. It seems unlikely that an analytic solution like the present one will be forthcoming.

In summary, complete solutions of the problem of ion collection by an arbitrary-shaped object have been obtained in the drift approximation (ignoring the polarization drift). The normalized flux density (67), (68) is a function only of the orientation of the surface, provided the object is convex. The precise meaning of "convex" here is that no positive characteristic that originates elsewhere on the object should pass through the point of interest. A transverse Mach probe using a variety of electrode orientations measures the $E \wedge B$ drift plus this specified combination of both ion and electron diamagnetic drifts. Its ideal calibration has been derived, and possible problems arising from finite size identified and quantified.

References

[1] I. H. Hutchinson, *Principles of Plasma Diagnostics* (Cambridge University Press, Cambridge, 2002), 2nd ed., chapter 3.

[2] P. K. Shukla and A. A. Mamun, *Introduction to Dusty Plasma Physics* (IOP Publishing, Bristol, 2002).

[3] D. Hastings and H. Garret, *Spacecraft-Environment Interactions* (Cambridge University Press, 2004).

[4] K.-U. Riemann, Phys. Plasmas **1**, 552 (1994).

[5] T. Daube and K.-U. Riemann, Phys. Plasmas **6**, 2409 (1999).

[6] S. Devaux and G. Manfredi, Phys. Plasmas **13**, 083504 (2006).

[7] I. H. Hutchinson, Phys. Fluids **30**, 3777 (1987).

[8] I. H. Hutchinson, Phys. Rev. A **37**, 4358 (1988).

[9] J. P. Gunn, C. Boucher, P. Devynck, I. Duran, K. Dyabilin, J. Horacek, M. Hron, J. Stockel, G. Van Oost, H. Van Goubergen, et al., Phys. Plasmas **8**, 1995 (2001).

[10] H. Van Goubergen, R. R. Weynants, S. Jachmich, M. Van Schoor, G. Van Oost, and E. Desoppere, Plasma Phys. Control. Fusion **41**, L17 (1999).

[11] I. H. Hutchinson, Phys. Plasmas **3**, 6 (1996).

[12] C. MacLatchy, C. Boucher, D. Poirier, and J. Gunn, Rev. Sci. Instrum. **63**, 3923 (1992).

[13] S. Gangadhara and B. LaBombard, Plasma Physics and Controlled Fusion **46**, 1617 (2004).

[14] P. Peleman, S. Jachmich, Y. Xu, C. Boucher, G. Van Oost, B. Schweer, and M. Mitri, Rev. Sci. Instrum. **77**, 10E710 (2006).

[15] J. Gunn, Czech. J. Phys. **48, S2**, 293 (1998).

[16] I. H. Hutchinson, Phys. Rev. Lett. **101**, 03500 (2008).

[17] I. H. Hutchinson, Phys. Fluids **31**, 2728 (1988).

[18] A. V. Chankin and P. C. Stangeby, Plasma Phys. Control. Fusion **36**, 1485 (1994).

[19] R. H. Cohen and D. D. Ryutov, Phys. Plasmas **2**, 2011 (1995).

[20] R. Courant and D. Hilbert, *Methods of Mathematical Physics*, vol. II (Wiley, Interscience, 1962), chap V.

[21] N. Smick and B. LaBombard, Bull. Amer. Phys. Soc. **51**, 243 (2006), [Division of Plasma Physics, paper QP1-66].

[22] R. Chodura, Phys. Fluids **25**, 1628 (1982).

[23] P. Peleman, S. Jachmich, M. Van Schoor, G. Van Oost, W. Knaepen, and C. Boucher, Contrib. Plasma Phys. p. 422 426 (2006).

[24] T. Shikama, S. Kado, A. Okamoto, S. Kajita, and S. Tanaka, Phys. Plasmas **12**, 044504 (2005).

[25] K.-S. Chung and I. H. Hutchinson, Phys. Rev. A **38**, 4721 (1988).